Graphene Oxide Nanoribbon as Hole Extraction Layer to Enhance Efficiency and Stability of Polymer Solar Cells

Jun Liu, Gi-Hwan Kim, Yuhua Xue, Jin Young Kim, Jong-Beom Baek, Michael Durstock, and Liming Dai*

Owing to its unique 2-dimensional carbon nanostructure with unique electrical, optical, thermal, and mechanical properties, graphene has attracted a great deal of interest.[1,2] While the pristine graphene is a zero-bandgap material with metal-like conductivity, graphene nanoribbon (GNR) is semiconducting with an opened bandgap induced by the quasi-one-dimensional confinement of charge carriers.[3–8] However, graphene and its nanoribbons without functionalization are insoluble and infusible. The poor processability has precluded the pristine graphene materials, including GNR, for various potential applications. This limitation has been circumvented by oxidizing graphene with acids (e.g., $H_2SO_4/KMnO_4$) to produce graphene oxide (GO) with oxygen-containing groups (e.g., –COOH, –OH) around and on the carbon basal plane,[2] leading to low-cost mass production of soluble graphene derivatives for potential applications. By introducing the oxygen-rich groups around a graphene nanoribbon, the resultant graphene oxide nanoribbon (GOR) should show a synergistic effect to have the bandgap of GNR and solution processability of GO. Therefore, GORs could be a new class of solution-processable semiconducting materials attractive for optoelectronic applications. In this study, we demonstrate, for the first time, that GOR can be used as an excellent hole-extraction material to significantly improve the performance of polymer solar cells (PSCs).

PSCs using polymeric materials to convert solar energy to electricity is an emerging photovoltaic technology to compete with the widely used photovoltaic technologies based on inorganic materials.[9] In spite of many advantages (e.g., low cost, flexibility, and semi-transparency), the efficiency and lifetime of PSCs are still largely limited by, among other factors, the poor charge extraction from the active layer to electrodes.[10,11] Thus,

a hole/electron extraction layer is often required to maximize the device efficiency. An ideal hole extraction material should have a proper energy level alignment to improve hole extraction and to selectively block electrons to diminish electron-hole recombination on anode. Moreover, the hole extraction material should also have solution processability and good film-forming property for low-cost device fabrication.[10,11] However, the widely used hole extraction layer (HEL), poly(3,4-ethylenedioxythiophene) doped with poly(styrenesulfonate) (PEDOT:PSS), suffers from poor device lifetime due to its acidic and hygroscopic nature[12] while other HELs, such as semiconducting metal oxides (e.g., NiO, MoO_3, V_2O_5), always need to be vacuum-deposited with a high manufacturing cost.[13–16] Although solution-processable GO has recently been used as the HEL with no obvious detrimental effect on the device lifetime, it suffers from low device efficiency owing to its unproper energy level alignment and insulating property.[17–22] Unlike the two-dimensional GO, the quasi-one-dimensional GOR possesses a proper energy level alignment, good solubility, and excellent film-forming capability. As demonstrated in this study, GOR surpasses the existing hole extraction materials, in terms of the device efficiency, stability, and manufacturing cost, to facilitate the development of high-performance PSCs.

As shown in **Scheme 1**, GOR was synthesized from oxidative unzipping of single-walled carbon nanotubes (SWCNTs) with $KMnO_4$ as oxidant in concentrated H_2SO_4. Slightly different from the published procedure,[8] in which 500 wt% $KMnO_4$ was used for unzipping of SWCNTs to afford graphene ribbons, we added extra 200 wt% $KMnO_4$ (0.4 equiv) after the unzipping process with 500 wt% $KMnO_4$ for further oxidization of GOR to generate additional defect sites on the GOR, and hence more bandgap opening. The additional oxidation process could also shorten the GOR. Upon completion of the oxidation reaction, the resultant GOR was purified by repeated centrifuging to remove the residual SWCNTs, if any (see Experimental Section). The purified GOR can be readily dispersed in water (>8 mg mL^{-1}) or other polar organic solvents (e.g., dimethylformamide).

Figure 1a shows a typical transmission electron microscopy (TEM) image for the resultant GOR having a width of about 8 nm and length of more than 100 nm. The corresponding atomic force microscopic (AFM) image shown in Figure 1b reveals that the GOR has a thickness of about 1 nm similar to that of a single-layer GO sheet.[23,24] TEM and AFM images taken from the GOR samples prepared from a concentrated aqueous solution (1 mg mL^{-1}) (Figures S1a and S1b, Supporting Information) indicate that the GOR tends to entangle in the solid state due to their large aspect ratio, good flexibility, and strong hydrogen bonding between the COOH/OH–containing GORs.

Dr. J. Liu, Dr. Y. Xue, Prof. L. Dai
Department of Macromolecular Science and Engineering
Case School of Engineering
Case Western Reserve University
10900 Euclid Avenue, Cleveland,
Ohio, 44106, USA
E-mail: liming.dai@case.edu
G.-H. Kim, Prof. J. Y. Kim, Prof. J.-B. Baek
Interdisciplinary School of Green Energy
Ulsan National Institute of Science and Technology (UNIST)
Ulsan, 689–798, Republic of Korea
Dr. M. Durstock
Materials and Manufacturing Directorate
Air Force Research Laboratory, RXBP
Wright-Patterson Air Force Base,
Ohio, 45433, USA

Report Documentation Page	*Form Approved* *OMB No. 0704-0188*

Public reporting burden for the collection of information is estimated to average 1 hour per response, including the time for reviewing instructions, searching existing data sources, gathering and maintaining the data needed, and completing and reviewing the collection of information. Send comments regarding this burden estimate or any other aspect of this collection of information, including suggestions for reducing this burden, to Washington Headquarters Services, Directorate for Information Operations and Reports, 1215 Jefferson Davis Highway, Suite 1204, Arlington VA 22202-4302. Respondents should be aware that notwithstanding any other provision of law, no person shall be subject to a penalty for failing to comply with a collection of information if it does not display a currently valid OMB control number.

1. REPORT DATE **2013**	2. REPORT TYPE	3. DATES COVERED **00-00-2013 to 00-00-2013**

4. TITLE AND SUBTITLE **Graphene Oxide Nanoribbon as Hole Extraction Layer to Enhance Efficiency and Stability of Polymer Solar Cells**	5a. CONTRACT NUMBER
	5b. GRANT NUMBER
	5c. PROGRAM ELEMENT NUMBER
6. AUTHOR(S)	5d. PROJECT NUMBER
	5e. TASK NUMBER
	5f. WORK UNIT NUMBER

7. PERFORMING ORGANIZATION NAME(S) AND ADDRESS(ES) **Case Western Reserve University,Department of Macromolecular Science and Engineering,10900 Euclid Avenue,Cleveland,OH,44106**	8. PERFORMING ORGANIZATION REPORT NUMBER

9. SPONSORING/MONITORING AGENCY NAME(S) AND ADDRESS(ES)	10. SPONSOR/MONITOR'S ACRONYM(S)
	11. SPONSOR/MONITOR'S REPORT NUMBER(S)

12. DISTRIBUTION/AVAILABILITY STATEMENT
Approved for public release; distribution unlimited

13. SUPPLEMENTARY NOTES

14. ABSTRACT

15. SUBJECT TERMS

16. SECURITY CLASSIFICATION OF:			17. LIMITATION OF ABSTRACT	18. NUMBER OF PAGES	19a. NAME OF RESPONSIBLE PERSON
a. REPORT **unclassified**	b. ABSTRACT **unclassified**	c. THIS PAGE **unclassified**	**Same as Report (SAR)**	**5**	

Standard Form 298 (Rev. 8-98)
Prescribed by ANSI Std Z39-18
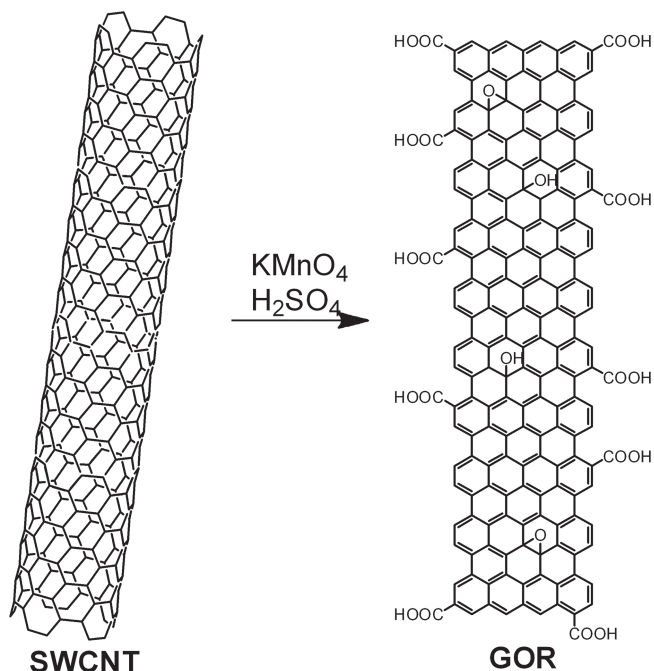
Scheme 1. Schematic illustration of synthesizing GOR from oxidative unzipping of SWCNTs.

Figure 1. TEM image (a), AFM image and height profile (b), XPS survey spectrum (c), and XPS C1s spectrum (d) of GOR.

The X-ray photoemission spectroscopic (XPS) survey spectrum of the GOR given in Figure 1c shows a significant amount of oxygen (24.9 at%). In a good consistence with Scheme 1, the presence of C–C, C–O (hydroxyl/epoxy) and COOH moieties in the GOR structure is clearly evident by the corresponding curve-fitted XPS C1s spectrum (Figure 1d). The much higher percentage of COOH groups in the XPS C1s spectrum of GOR (11.6 at%) than that reported for GO (ca. 3 at%),[23,24] is attributable to the large aspect ratio of the edge-carboxylated GOR.

GOR is amorphous in solid state, as evidenced by the absence of diffraction peak in our X-ray diffraction (XRD) profiles (Figure S2). Unlike GO that is semicrystalline with diffraction peaks arising from its layered structure in the solid state,[23,24] therefore, the entanglement of GOR has prevented the face-to-face stacking of the GOR basal plane, leading to an amorphous state. As a result, GOR can readily form a uniform and smooth film by simple spincoating. **Figure 2** shows the AFM height and phase images for a bare ITO surface before and after spincoating with an aqueous solution of GOR (3 mg mL^{-1}). Owing to the rough surface of ITO, the deposition of a thin GOR film causes no obvious change in its height image (Figures 2a and 2b). The root mean square (rms) roughness of the AFM height image after GOR spincoating (3.46 nm) is quite close to that (3.86 nm) of the bare ITO surface. However, the corresponding phase image of the GOR-coated ITO (Figure 2d) become much more uniform than that of the bare ITO surface (Figure 2c), indicating the presence of a uniform and thin GOR layer. The observed excellent film forming property of GOR is a good advantage for its application as HEL in PSCs[10,11] (vide infra). The uniformity of the GOR film will be analyzed in future studies.
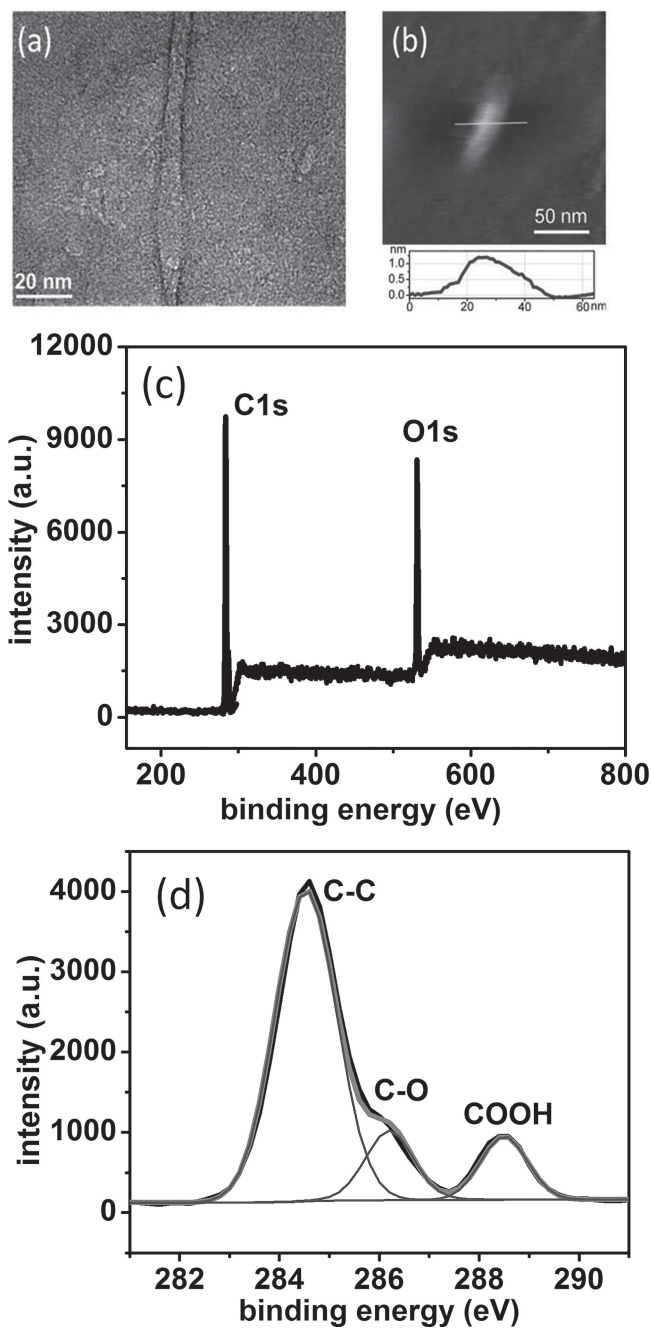
Cyclic voltammetry (CV) has been routinely used to determine the LUMO and HOMO levels of organic molecules and polymers. Since GOR can be regarded as a quasi-one-dimensional polymer, we adopted CV to investigate the LUMO/HOMO energy levels of GOR. As shown in **Figure 3**a, both reduction and oxidation peaks are evident in the cyclic voltammetry (CV) of the GOR film. According to the onset potential of the reduction and oxidation process, the LUMO and HOMO energy levels of GOR are estimated from the formula ($E_{LUMO} = -e$ (E_{red} + 4.4) [eV], $E_{HOMO} = -e$ (E_{ox}+ 4.4) [eV])[25] to be −3.5 eV and −5.0

Materials
Views
www.MaterialsViews.com

ADVANCED
MATERIALS
www.advmat.de

COMMUNICATION
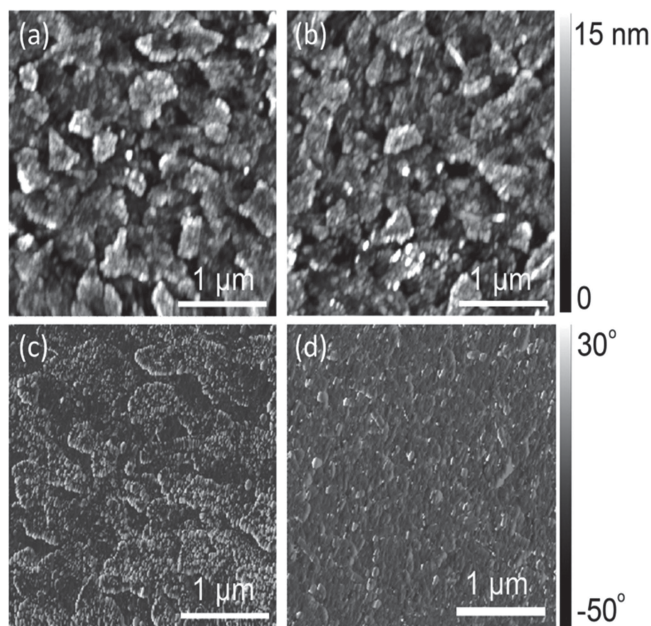
Figure 2. AFM height and phase images of ITO glass before (a,c) and after (b,d) being spincoated with GOR.

Figure 3. Cyclic voltammetry (a) and UV/Vis absorption spectrum (b) of GOR.

eV, respectively. Thus, the electrochemical bandgap of GOR is 1.5 eV. More importantly, the HOMO level of GOR is very close to that of the donor material, poly(3-hexylthiophene) (P3HT), which can improve hole extraction (**Figure 4**a). Besides, the relatively large energy barrier between the LUMO of GOR and that of the acceptor material, phenyl-C_{61}-butyric acid methyl ester (PCBM), can effectively block electrons to minimize possible charge combination loss at the anode. Therefore, GOR possesses desirable energy levels for efficient hole extraction. Figure 3b reproduces a typical UV/Vis absorption spectrum of a GOR film on quartz, showing an absorption peak at 234 nm with an onset absorption wavelength at around 800 nm equivalent to an optical bandgap of about 1.5 eV in a good consistence with the electrochemical bandgap. The weak absorption in the visible range is an additional advantage for the use of GOR as HEL since its high transparency in the visible range allows for more efficient solar absorption by the active layer in PSCs.

To further test the performance of GOR as HEL in PSCs, we fabricated PSC devices based on the widely-studied P3HT:PCBM bulk heterojunction active layer with the structure of ITO/HEL/P3HT:PCBM (200 nm)/Ca (20 nm)/Al (100 nm) without and with PEDOT:PSS, GO or GOR as the HEL (see Figure 4b). The GOR layer was deposited by spincoating from its aqueous solution with a concentration of 3 mg mL^{-1} to give a thickness of about 1 nm. We have tested the GOR concentration from 1 mg mL^{-1} to 8 mg mL^{-1} and found that 3 mg mL^{-1} gave the best device performance. Figures 4c and 4d show the current density-voltage (*J-V*) and the external quantum efficiency (EQE) curves, respectively, measured from these devices under AM1.5G illumination. As can be seen, the device with GO as the HEL exhibits an open-circuit voltage (V_{OC}) of 0.62 V, short-circuit current density (J_{SC}) of 8.42 mA cm^{-2}, fill factor (FF) of 0.60, and power conversion efficiency (PCE) of
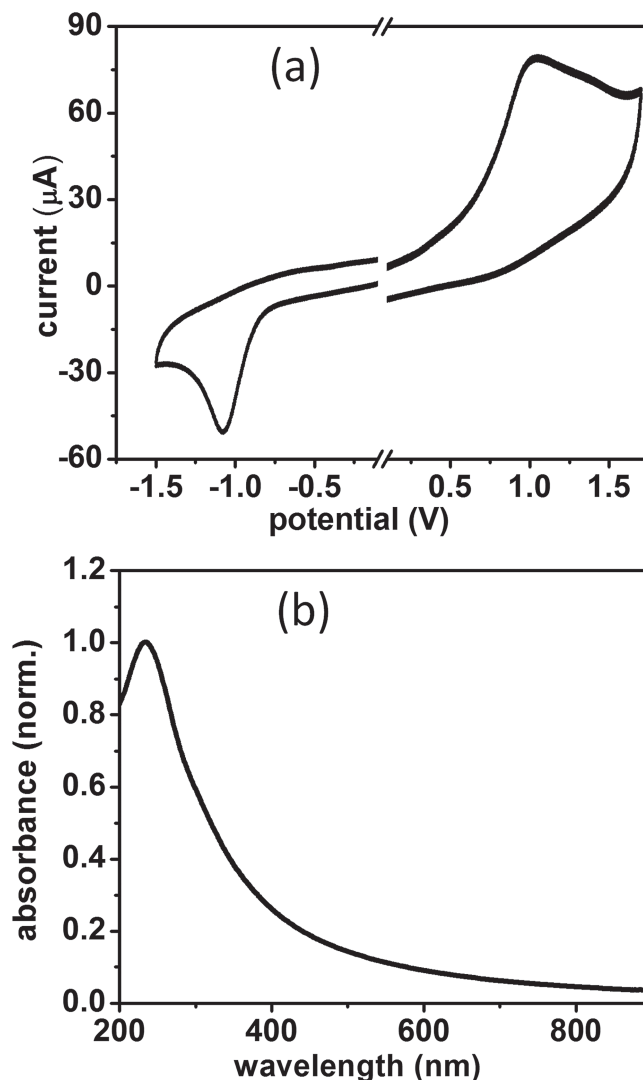
3.08%. This performance is much better than that of the corresponding device based on the bare ITO without HEL. When GOR was used as HEL, the device shows a V_{OC} of 0.62 V, J_{SC} of 9.96 mA cm^{-2}, FF of 0.67, and PCE of 4.14%. The much better performance of the GOR-based device than its GO-counterpart indicates that GOR is an excellent hole extraction material for PSCs. **Table 1** lists the numerical performance data, along with the corresponding series resistance (R_S) and shunt resistance (R_{SH}). Compared with the GO-based device, the GOR-based device exhibits a lower R_S and a higher R_{SH}. In view of the energy level alignment shown in Figure 4a, we attribute the excellent performance for the GOR-based device to the improved hole extraction and electron blocking capabilities. In addition, the formation of a thin and uniform film of GOR on the ITO electrode offers an additional advantage for the PSC application. Both the proper energy level alignment and the excellent film forming property of GOR contribute to the observed excellent device performance.
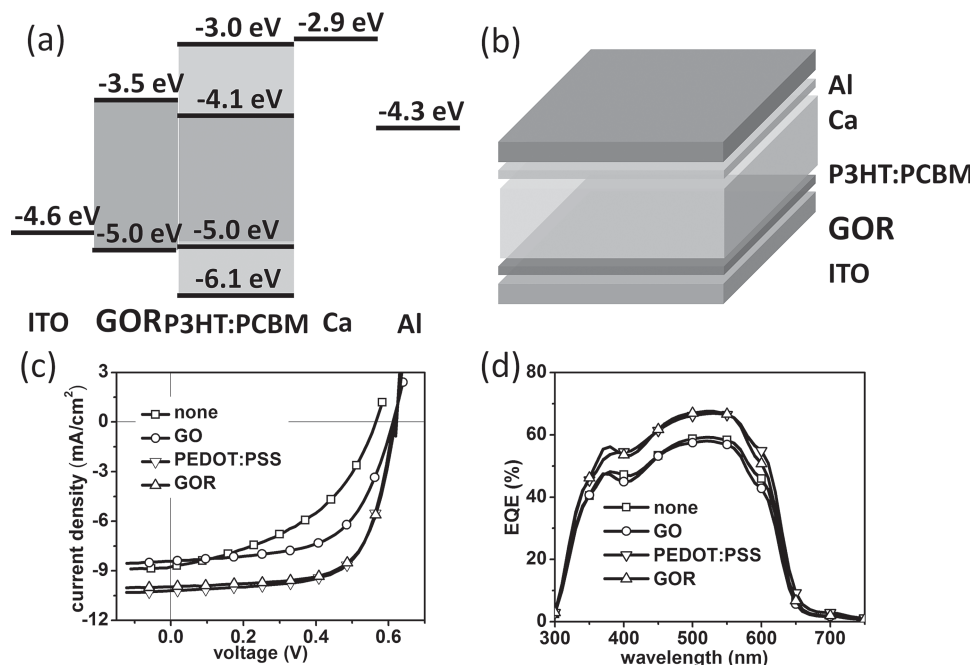
**ADVANCED
MATERIALS**

www.advmat.de

COMMUNICATION

*Materials
Views*

www.MaterialsViews.com

Figure 4. Device energy level alignment (a) and device structure (b) of the GOR-based PSC device. Current density-voltage (J-V) curves (c) and EQE curves (d) under AM1.5G illumination of the PSCs without and with PEDOT:PSS, GO or GOR as the HEL.

As mentioned earlier, the conventional PEDOT:PSS HEL suffers from poor device stability due to its acidic and hygroscopic nature.[12] To test the stability of the GOR-based device, we studied two PSCs with the configuration of ITO/PEDOT:PSS or GOR/P3HT:PCBM (200 nm)/Al (100 nm). For the stability study, Ca was eliminated because Ca was too sensitive to oxygen and moisture. The device performance was recorded as a function of storage time in a N_2-filled glovebox without any device encapsulation. As shown in **Figure 5**, the PCE of the PEDOT:PSS-based device drops to 75% of its original value after storage for 90 days. In contrast, the GOR-based device remains 86% of the original value under the same condition, suggesting that GOR is a more stable hole extraction interfacial layer than PEDOT:PSS.

In summary, we have demonstrated, for the first time, that GOR possesses proper energy level alignment, good solubility, and excellent film-forming propertie to be an excellent hole extraction material to enhance efficiency and stability of PSCs. PSC devices based on the GOR HEL outperform their counterparts based on conventional hole extraction materials, including PEDOT:PSS. The unique structure, interesting properties and

excellent device performance of GOR offer a new pathway for the development of novel carbon nanomaterials for high-performance PSCs.

Experimental Section

Synthesis and Purification of GOR: GOR was prepared according to the published procedure.[7,8] To start with, SWCNTs (from Cheap tubes Inc.) were subjected to thermal annealing at 220 °C in humid air atmosphere overnight, and then were washed with hydrochloric acid to remove the catalyst residual. Thereafter, the SWCNTs were rinsed sequentially with aqueous Na_2CO_3, H_2O, and methanol, followed by dried at 50 °C

Table 1. Characteristics of the PSC devices without or with different HEL under AM1.5G illumination.

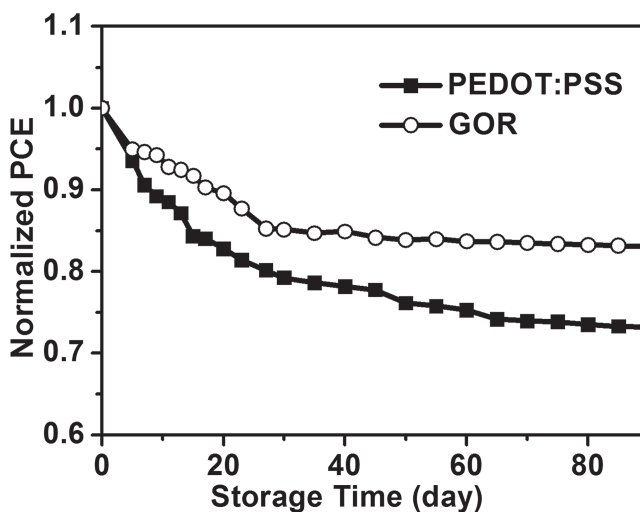| HEL	V_{OC} (V)	J_{SC} (mA cm^{-2})	FF	PCE (%)	PCE[a] (%)	R_s (Ω cm^2)	R_{sh} (Ω cm^2)
none	0.56	8.75	0.45	2.20	2.06 ± 0.20	18.37	194
GO	0.62	8.42	0.60	3.08	2.86 ± 0.42	12.50	696
PEDOT:PSS	0.61	10.10	0.68	4.19	4.16 ± 0.23	6.59	958
GOR	0.62	9.96	0.67	4.14	4.02 ± 0.29	6.75	945

[a]average PCE and deviation of nine devices.

Figure 5. PCE decay of a PEDOT:PSS-based device and a GOR-based device unencapsulated and stored in a N_2-filled glovebox.

overnight. A mixture of the purified SWCNTs (100 mg) and 98% H_2SO_4 (150 mL) was ultrasonicated in a water bath for 20 minutes and stirred overnight at room temperature. To the SWCNT dispersion, $KMnO_4$ (500 mg) was then added in five portions and stirred at room temperature for 2 hours. After the resulting mixture was stirred at 70 °C for two more hours, extra $KMnO_4$ (200 mg) was added in several portions, which was accompanied by color change from dark to light violet-red. Upon cooling down to room temperature, the reaction mixture was carefully poured into a mixture of 400 g ice, 50 g water, and 5 mL H_2O_2 under stirring. Finally, the resultant dispersion was centrifuged (22000 rpm, 20 min) to give crude GOR as dark precipitate (110 mg).

Our AFM and TEM measurements indicated that the crude GOR product contained a high content of residual SWCNTs in a bundle form or complexed with the GOR. So, tedious centrifuging was performed to remove the residual SWCNTs. To start with, the crude GOR (30 mg) was dispersed in water (20 mL) and one drop of hydrochloric acid, followed by filtration through 0.2 μm membrane to remove inorganic impurities. The collected solid was then redispersed in water (20 mL) and centrifuged at 6000 rpm for 20 minutes. The precipitate (most probably SWCNT bundles) was discarded. To the supernant, ammonium hydroxide (2 mL) was added, followed by bath ultrasonication for 30 minutes for dissociating GOR and SWCNTs. The resulting dispersion was centrifuged at 20000 rpm for 20 minutes to remove the black precipitate. The supernant was collected, to which hydrochloric acid was added to tune the pH = 2 for precipitation of the purified GOR. The dispersion was further centrifuged at 20000 rpm for 20 minutes and the black precipitate was collected as the purified GOR. The solid was further put on a 0.2 μm membrane and washed sequentially with water and methanol. Finally, the solid was dried at 35 °C in vacuum for two hours. The yield of the purified GOR was 18 mg (60%).

Device Fabrication and Measurements: ITO glass substrates were cleaned sequentially with detergent, de-ionized water, acetone, and *iso*-propanol, followed by drying with N_2 flow and UV-ozone treatment for 15 minutes. Then, the HEL was spincoated as follows. GO was spincoated from its 1 mg mL^{-1} aqueous solution at 2000 rpm for 60 s. GOR was spincoated from its 3 mg mL^{-1} aqueous solution at 2000 rpm for 60 s. PEDOT:PSS was spincoated from the solution (Al4083 from H. C. Starck) at 5000 rpm for 40 s, followed by heating at 140 °C for 10 minutes. After spincoating HEL, the device was transferred to a N_2-filled glovebox. Then, the active layer was spin-coated from the solution of P3HT/PCBM = 1/1 in o-dichlorobenzene (17 mg mL^{-1}) at 600 rpm for 60 s, followed by thermal annealing at 120 °C for 10 minutes. Finally, the device was transferred to a vacuum chamber for deposition of Ca (20 nm) and Al (100 nm) by thermal evaporation at a pressure of 10^{-7} Torr. The area of each device was 0.12 cm^2, as determined by the overlap of the ITO and the evaporated Al. All the devices were tested in a N_2-filled glovebox using a Keithley 2400 source meter and a Newport Oriel sol 2A solar simulator (300 W). The light intensity was calibrated to be 100 mW/cm^2 using a calibrated Si solar cell and a KG5 color filter. The device parameters were obtained from the current-voltage curves of the devices under illumination. The external quantum efficiency was recorded by a Solar Cell Measurement System from PV measurement Inc.

Supporting Information

Supporting Information is available from the Wiley Online Library or from the author.

[1] K. S. Novoselov, A. K. Geim, S. V. Morozov, D. Jiang, Y. Zhang, S. V. Dubonos, I. V. Grigorieva, A. A. Firsov, *Science* **2004**, *306*, 666.
[2] M. J. Allen, V. C. Tung, R. B. Kaner, *Chem. Rev.* **2010**, *110*, 132.
[3] Y.-W. Son, M. L. Cohen, S. G. Louie, *Phys. Rev. Lett.* **2006**, *97*, 216803.
[4] M. Y. Han, B. Özyilmaz, Y. Zhang, P. Kim, *Phys. Rev. Lett.* **2007**, *98*, 206805.
[5] X. Li, X. Wang, L. Zhang, S. Lee, H. Dai, *Science* **2008**, *319*, 1229.
[6] L. Xie, H. Wang, C. Jin, X. Wang, L. Jiao, K. Suenaga, H. Dai, *J. Am. Chem. Soc.* **2011**, *133*, 10394.
[7] D. V. Kosynkin, W. Lu, A. Sinitskii, G. Pera, Z. Sun, J. M. Tour, *ACS Nano* **2011**, *5*, 968.
[8] D. V. Kosynkin, A. L. Higginbotham, A. Sinitskii, J. R. Lomeda, A. Dimiev, B. K. Price, J. M. Tour, *Nature* **2009**, *458*, 872.
[9] G. Yu, J. Gao, J. C. Hummelen, F. Wudl, A. J. Heeger, *Science* **1995**, *270*, 1789.
[10] R. Steim, F. R. Koglera, C. J. Brabec, *J. Mater. Chem.* **2010**, *20*, 2499.
[11] H.-L. Yip, A. K.-Y. Jen, *Energy Environ. Sci.* **2012**, *5*, 5994.
[12] Y.-H. Kim, S.-H. Lee, J. Noh, S.-H. Han, *Thin Solid Films* **2006**, *510*, 305.
[13] V. Shrotriya, G. Li, Y. Yao, C. W. Chu, Y. Yang, *Appl. Phys. Lett.* **2006**, *88*, 073508.
[14] M. D. Irwin, D. B. Buchholz, A. W. Hains, R. P. H. Chang, T. J. Marks, *PNAS* **2008**, *105*, 2753.
[15] S. Murase, Y. Yang, *Adv. Mater.*, **2012**, *24*, 2459.
[16] J. J. Jasieniak, J. Seifter, J. Jo, T. Mates, A. J. Heeger, *Adv. Funct. Mater.* **2012**, *22*, 2594.
[17] J. Liu, Y. H. Xue, Y. X. Gao, D. S. Yu, M. Durstock, L. Dai, *Adv. Mater.* **2012**, *24*, 2228.
[18] J. Liu, Y. Xue, L. Dai, *J. Phys. Chem. Lett.* **2012**, *3*, 1928.
[19] S. S. Li, K. H. Tu, C. C. Lin, C. W. Chen, M. Chhowalla, *ACS Nano* **2010**, *4*, 3169.
[20] S. Yeo, J. Kim, H.-G. Jeong, D.-Y. Kim, Y.-J. Noh, S.-S. Kim, B.-C. Ku, S.-I. Na, *Adv. Mater.* **2011**, *23*, 4923.
[21] Y. Gao, H. L. Yip, S. K. Hau, K. M. O'Malley, N. Cho, H. Z. Chen, A. K. Y. Jen, *Appl. Phys. Lett.* **2010**, *97*, 203306.
[22] J. Kim, V.-C. Tung, J. X. Huang, *Adv. Energy Mater.* **2011**, *1*, 1052.
[23] Y. W. Zhu, S. Murali, W. W. Cai, X. S. Li, J. W. Suk, J. R. Potts, R. S. Ruoff, *Adv. Mater.* **2010**, *22*, 3906.
[24] Y. Xue, H. Chen, D. S. Yu, S. Wang, M. Yardeni, Q. Dai, Y. Liu, J. Qu, L. Dai, *Chem. Comm.* **2011**, *47*, 11689.
[25] A. J. Bard, L. A. Faulkner, *Electrochemical Methods-Fundamentals and Applications* Wiley, New York **1984**.